JOURNAL OF GEOPHYSICAL RESEARCH, VOL. 99, NO. A1, PAGES 449–458, JANUARY 1, 1994

Space charge enhanced, plasma gradient induced error in satellite electric field measurements

D. A. Diebold, N. Hershkowitz, J. R. DeKock, T. P. Intrator, and S-G. Lee
Department of Nuclear Engineering and Engineering Physics, University of Wisconsin, Madison

M-K. Hsieh
Department of Electrical and Computer Engineering, University of Wisconsin, Madison

Abstract. In magnetospheric plasmas it is possible for plasma gradients to cause error in electric field measurements made by satellite double probes. The space charge enhanced plasma gradient induced error is discussed in general terms, the results of a laboratory experiment designed to illustrate this error are presented, and a simple expression that quantifies this error in a form that is readily applicable to satellite data is derived. The simple expression indicates that for a given probe bias current there is less error for cylindrical probes than for spherical probes. The expression also suggests that for Viking data the error is negligible.

Introduction

Measurements of electric fields in the magnetosphere are often made by cylindrical or spherical satellite double probes. Plasma gradients are known to exist in the magnetosphere, and it has been recognized for some time [*Fahleson*, 1967] that plasma gradients can cause error in electric field measurements made by satellite double probes [*Aggson and Heppner*, 1964, *Boyd*, 1967]. In this paper we investigate space charge enhanced, plasma gradient induced error in satellite double-probe electric field measurements.

Figure 1*a* is a simplified schematic of a satellite—double-probe system. As a matter of convenience, spherical probes are depicted; but the arguments presented in this paper apply equally as well to cylindrical probes. Cylindrical probes tend to have a different high-frequency response than spherical probes [*Gurnett*, 1991]; and if their lengths are comparable to the distance of probe separation, they tend to spatially integrate. These aspects of probe behavior are not considered in this paper. Only low-frequency phenomena are considered, and any spatial integration effects that are due to long cylindrical probe lengths are ignored.

The size of the probes and the satellite shown in Figure 1*a* have been exaggerated for clarity. The probes are conductors and are electrically isolated from the booms. The voltage difference between the probes divided by the distance between the probes is the double-probe measurement of the average electric field in the ambient plasma [see *Pedersen et al.*, 1978].

Probe voltage is not necessarily, and most often is not, equal to the ambient plasma potential. The difference between the probe voltage and the nearby ambient plasma potential is referred to as the sheath potential. When the sheath potentials of the two probes of a double probe are equal, the sheath potentials cancel one another in the calculation of electric field and the double-probe measurement is accurate. However, when the sheath potentials are not equal, they do not cancel and there is error in the double-probe technique [*Pedersen et al.*, 1984]. This error is equal to the difference in sheath potentials divided by the distance between probes.

Figure 1*b* shows the qualitative potential structure associated with the satellite—double-probe system when there is no significant error in the double-probe technique, i.e., when the sheath potentials of the two probes are equal. For a situation such as that depicted in Figure 1*c*, there is error in the double-probe technique because the sheath potentials of the two probes are not equal. For the particular case shown, the electric field in the ambient plasma is less than that suggested by the double-probe technique.

Differences in sheath potentials can be caused by differences between probes. To minimize the error caused by these differences, both probes of a double probe are built to be as identical as possible. In addition, care is taken to ensure that probe surface properties are uniform. For example, conducting materials are used for probe surfaces so that the surfaces are equipotential [*Mozer et al.*, 1978].

Because magnetospheric plasmas tend to be tenuous, photoemission can dominate the currents flowing between probes and magnetospheric plasmas. Hence, in the magnetosphere, probe photoemissive properties can be of particular importance; and further steps are often taken to ensure that the photoemission from both probes of magnetospheric double probes are equal. For example, when making a magnetospheric double probe, structures near the probes (such as booms and guards) are usually constructed in such a way that both probes are equally shadowed for all spin angles [*Fehringer*, 1989]. Also, negatively biased guards are often placed between the probes and the satellite to minimize leakage currents and their effects [*Mozer et al.*, 1978]. Photoemission leakage currents are those photoelectric currents that flow directly between the probes and the satellite without passing through ambient plasma. When the photoemissive leakage currents of the two probes are not equal, spurious sunward electric field measurements are usually the result [*Pedersen et al.*, 1984].

Implementation of the methods mentioned above can

Paper number 93JA00432.
0148-0227/94/93JA-00432$05.00

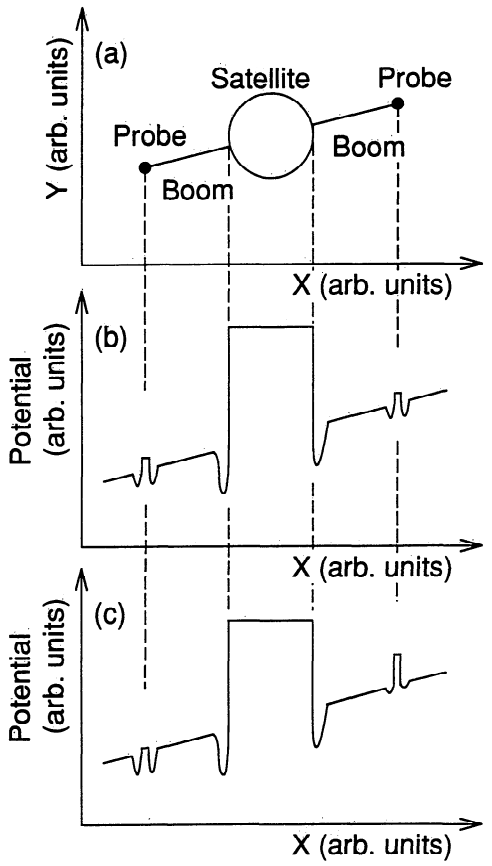

Figure 1. (*a*) A simplified schematic of a satellite–double-probe system. The size of the probes and the satellite shown are exaggerated for clarity. As a matter of convenience, spherical probes are depicted; but the arguments presented in the text apply to cylindrical probes as well. (*b*) The qualitative potential structure associated with the satellite–double-probe system when there is no significant error in the double-probe technique. (*c*) The potential structure when there is error.

reduce the differences in probes, and their photoemissive currents, considerably. Even so, the voltages and sheath potentials of electrically isolated or floating probes in tenuous magnetospheric plasmas can be extremely sensitive to currents because of the very large sheath impedances of the probes. Consequently, current sources are also often essential in obtaining good double-probe measurements in magnetospheric plasmas [*Pedersen et al.*, 1978]. When current sources are used, probes are said to be "current biased." Current sources force equal net electrical or "bias" currents to flow from each probe of a double probe to the satellite and thereby reduce probe sheath impedances. As a result, when probes are current biased, spurious currents produce smaller excursions of probe voltages, smaller changes in sheath potentials and less error in double-probe measurements.

Besides differences in probes and their photoemissive currents, sheath potential differences can also be caused by differences in the ambient plasmas surrounding probes. Error in the double-probe technique that is caused by differences in the ambient plasmas at each probe of a double probe that are due to gradients in the ambient plasma will be referred to in this paper as plasma gradient induced error (PGIE). The scope of this paper is restricted to space charge enhanced PGIE of current biased double-probe measurements made in tenuous plasmas such as those typically found in the magnetosphere.

Bias Current I_B and the Current Sources

The bias current I_B is the current that is forced by current sources to flow from each probe to the satellite in a double-probe—satellite system; and it is approximately the net current that flows to and from each probe from the ambient ions and electrons and from photoemission when error currents such as leakage currents are small, i.e., much less than I_B. Figure 2 shows the complete circuit for I_B, assuming the error currents are small. In order for currents to flow as shown in Figure 2, the satellite's potential must in general be greater than both the ambient plasma potential near the satellite and the probe potentials. Power must be provided to keep the currents flowing, and it is the current sources that provide this power.

The current sources adjust the voltage difference between each probe and the satellite until I_B flows from each probe to the satellite. In doing so, the current sources change the voltages of both the probes and the satellite. Since the ambient plasma potentials at both the probes and the satellite are fixed, the probe and satellite sheath potentials change when the probe and satellite voltages change. In effect, by changing the probe and satellite voltages, the current source changes the probe and satellite sheath potentials until I_B flows through each probe and $2I_B$ flows through the satellite.

Space Charge and Its Effects on Photoemitted Current

Space charge refers to net electric charge in a space or region. Space charge associated with photoemitted electrons exists near probes and satellites because of the finite velocity of photoemitted electrons and hence the finite time it takes photoemitted electrons to cross probe and satellite sheaths. This photoemitted space charge can be especially important in tenuous magnetospheric plasmas that may not be able to provide much space charge of their own at probes and satellites. Specifically, in tenuous plasmas the space charge associated with photoemitted electrons can cause local potential minima [*Guernsey and Fu*, 1970], such as those shown in Figure 1, near photoemitting probes and satellites.

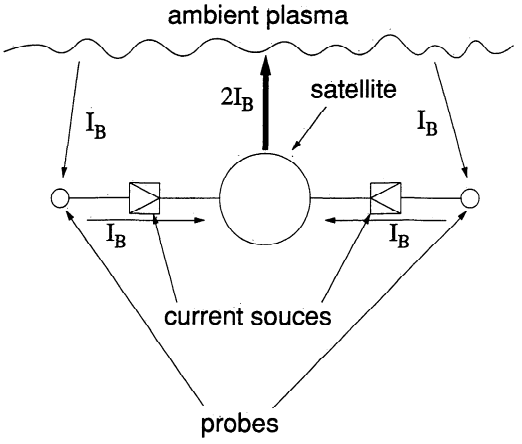

Figure 2. The complete circuit for the bias current I_B, when error currents can be ignored.

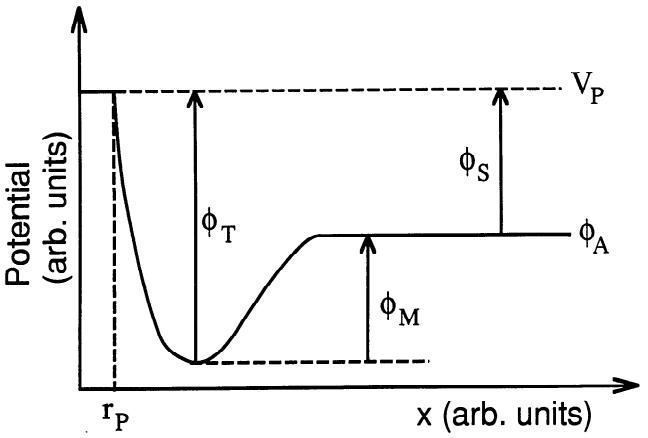

Figure 3. A qualitative illustration of the potential (arbitrary units) versus radius (arbitrary) near a photoemitting probe which shows the relationship between the probe voltage V_P, trapping potential ϕ_T, the sheath potential ϕ_S, the ambient plasma potential ϕ_A, and the difference ϕ_M between the ambient potential and the potential minimum. The probe radius is r_P.

Space charge associated with photoemitted electrons modifies probe and satellite sheaths in such a way as to tend to repel photoemitted electrons and force them back to the probe or satellite from which they were emitted. That is to say, electrons that are photoemitted from a probe or satellite tend to be repelled back to that probe or satellite by previously photoemitted electrons that are still in the probe or satellite sheath. As a result, because of this space charge, not every electron that is photoemitted from a probe or satellite necessarily escapes from that probe or satellite.

In calculations of current balance at a probe or satellite, the photoemitted electron current that leaves and then returns to that probe or satellite cancels itself and can be ignored. It is only the photoemitted current that escapes (leaves and does not return to) that probe or satellite that is important in such calculations. Here we will refer to electrical currents associated with all the electrons photoemitted from the probe as the photoemitted current I_P, the photoemitted electrons that escape a probe as the untrapped photoemitted current I_U, the photoemitted electrons that return to a probe as the trapped photoemitted current I_T, and the ambient plasma particles collected by a probe as the collected current I_C.

Note that $I_P = I_U + I_T$ and $I_U + I_C \simeq I_B$, where I_B is the bias current, which is approximately the current that flows from the ambient plasma to a probe when error currents are small and is also the current forced to flow from a probe to a satellite by a current source. Also note that $I_U = I_P \exp(-e\phi_T/T_e)$, where T_e is the temperature of the emitted electrons and ϕ_T is what we will refer to as the trapping potential. When a local minimum in potential exists near a probe because of the space charge associated with the electrons that are photoemitted from that probe, ϕ_T is the difference between the probe voltage V_p and the plasma potential at the minimum (see Figure 3). If the difference between the nearby ambient plasma potential ϕ_A and the plasma potential at the minimum, when it exists, is defined to be ϕ_M, then $\phi_T = \phi_S + \phi_M$, where ϕ_S is the sheath potential, which is the difference between the probe voltage and the nearby ambient plasma potential. When there is no local minimum near a probe, $\phi_T = \phi_S$. Hence a general expression for ϕ_T is $\phi_T = \phi_S + \phi_M$, with the understanding that ϕ_M is set to zero when there is no local minimum near a probe.

As noted in the introduction, differences in the sheath potentials ϕ_S of the two probes of a double-probe—satellite system cause error in the double-probe method. If the ϕ_S of the two probes are equal, then the ϕ_S subtract out of the double-probe electric field calculation and there is no error in the double-probe technique. Since $\phi_S = \phi_T - \phi_M$, differences in either ϕ_T or ϕ_M (or both) lead to error.

Space Charge Enhanced PGIE

When gradients in the ambient plasma exist and either $\phi_M = 0$ or the space charge associated with the photoemitted electrons of a probe, and hence ϕ_M also, is insensitive to ambient plasma parameters, the plasma gradient induced error PGIE in the double-probe method is due to gradient-induced differences in the ϕ_T of the two probes employed. However, when plasma gradients exist, ϕ_M is nonzero, and the space charge associated with the photoemitted electrons of a probe, and hence ϕ_M also, is sensitive to ambient plasma parameters, the plasma gradient induced error PGIE in the double-probe method is due to gradient-induced differences in both the ϕ_T and the ϕ_M of the two probes employed. This additional error that is due to the gradient-induced differences in the ϕ_M is what we refer to in this paper as the space charge enhanced PGIE.

Relatively small amounts of plasma can have rather large effects on space charge [*Kingdon*, 1923]. Plasma ions are attracted to the negative space charge of emitted electrons near a probe. Ions can spend relatively long periods of time orbiting the probe, and alleviating the negative space charge near the probe, because of the conservation of angular momentum. If there are not enough plasma ions to noticeably alleviate the space charge associated with emitted electrons near a probe, then the plasma is too tenuous for significant space charge enhanced PGIE. On the other hand, if there are enough plasma ions to completely alleviate the space charge, for example, I_C roughly $\geq I_U$, then the plasma is too dense for significant space charge enhanced PGIE.

For a hypothetical example of space charge enhanced PGIE, consider the situation depicted in Figure 1*c*. The deeper potential wells shown near the probe on the left-hand side of Figure 1*c*, as compared to the probe on the right, indicate a greater space charge near the left-hand probe. A gradient in plasma density, such that the ambient density near the probe on the right is greater than that near the probe on the left, could produce a difference in space charge near the two probes similar to that shown in Figure 1*c*. It is assumed that I_P and I_B are the same for each probe shown in Figure 1. To overcome the greater space charge and maintain I_B, the ϕ_S of the left-hand probe must be less than the ϕ_S of the probe on the right. Hence, for the situation shown in Figure 1*c*, the double-probe measured electric field would be greater than the actual electric field in the ambient plasma because of the greater space charge near the left-hand probe caused by the gradient in density, because of space charge enhanced PGIE.

Note that for the situation shown in Figure 1*c* the space charge associated with the electrons that are photoemitted

from the satellite does not enter into considerations of double-probe error. However, in some situations these electrons can affect the potentials at the probes; and, because of the asymmetry caused by the absence of photoemission from shadowed satellite surfaces, in such situations electrons photoemitted from the satellite can cause error. This type of error, which has been considered elsewhere [see *Aggson*, 1983], will not be considered here and is not the "space charge enhanced PGIE," which we refer to here.

Also, in this paper (and in Figure 1*c*), it is assumed that the ambient electric field is not large enough to alleviate space charge. *Borovsky* [1986] considered potential structures with potential drops much larger than the temperature of the ambient particles and found that although space charge effects were relatively unimportant other effects caused considerable error in the double-probe technique.

Laboratory Experiment

A laboratory experiment was conducted to illustrate space charge enhanced PGIE in a tenuous plasma. The experimental conditions were, of course, not the same as those found in the magnetosphere. However, efforts were made to ensure that the experimental conditions were such that the relevant physics of the experiment applied as well to magnetospheric conditions.

Apparatus and Technique

As a matter of convenience, a cylindrical, thermionically emitting probe 55 cm in length and 1.3×10^{-2} cm in diameter was employed in a cylindrical, stainless steel chamber that was 64 cm in length and 60 cm in diameter. The ratios of our probe's radius and length to the chamber's radius are approximately within the same order of magnitude as the corresponding ratios of the radii and lengths of satellite cylindrical double probes to magnetospheric Debye lengths. Also, the current emitted by our probe ($\sim$10 μA) is roughly within 2 or 3 orders of magnitude of the currents emitted by satellite double probes (e.g., the bias currents used for the GEOS 1 and Viking probes were approximately 80 nA [*Pedersen et al.*, 1978] and 150 nA (R. Boström, private communication, 1991), respectively). In the theory section it will be shown that the space charge enhanced PGIE depends on probe current, rather than probe current per unit length or area.

Our probe was heated into thermionic emission by a variable, half-wave rectified, 60-Hz heating voltage. Voltage bias sweeps between -10 and 5 V were applied to the probe through a CA3140E operational amplifier that was configured as a voltage follower. An ORTEC Brookdeal 9415 linear gate was employed to take data during the off cycle of the heating voltage. These voltage bias sweeps allowed probe current versus voltage characteristics to be measured under a variety of conditions.

Plasma could be created by bleeding air into the machine until the pressure reached the 10^{-3} torr range. The voltage drop across the probe during the on part of the heating cycle was large enough that some of the electrons were emitted with enough energy to ionize. Once plasma had been created in the 10^{-3} torr range, plasma could be produced at lower pressure (as low as approximately 1×10^{-4} torr). The plasma density was roughly proportional to the neutral pressure and was very roughly in the 10^3 to 10^5 cm^{-3} range. The plasma electron temperature was approximately 2 eV.

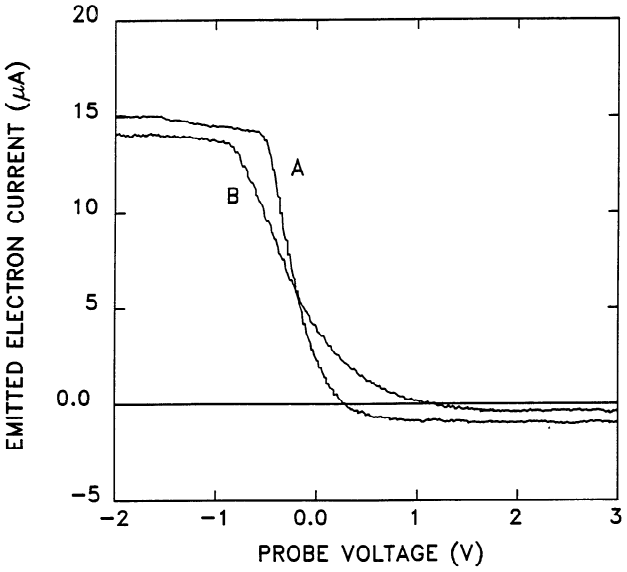

Figure 4. The data labeled as *A* and *B* are two current (microamperes) versus voltage (volts) characteristics measured from the same laboratory probe under different plasma and probe conditions.

Three problems made the measurements difficult. The origin of all three problems was the finite impedance between the primary and secondary of the heating voltage transformer. The currents that flowed through the transformer's finite impedance also flowed through our measuring apparatus and thus were a source of error. The three problems and our solutions to them are discussed in detail in Appendix A.

Laboratory Results

Figure 4 shows the laboratory data illustrate space charge enhanced PGIE. In Figure 4, current that is associated with electrons that are emitted from the probe and do not return to the probe is shown as positive current. The negative current at positive potentials indicates net collected electron current. The current versus voltage characteristics *A* and *B* shown in Figure 4 are characteristics of the same laboratory probe taken under different probe and plasma conditions. Specifically, probe emission was stronger and, more importantly, the plasma was more dense when characteristic *A* was taken.

Let us assume for the purpose of an illustration of space charge enhanced PGIE that characteristics *A* and *B* are the characteristics of two probes on a satellite that are being used to make electric field measurements. Again, the standard double-probe method for calculating average electric field is to divide the measured voltage differences between the probes by the distance between the probes.

Using this standard method, the electric field calculated from characteristics *A* and *B* depends on the current bias that is chosen. Most strikingly, characteristics A and B suggest that under "certain conditions," measurements would indicate a positive, zero, or negative electric field depending on the current bias that is chosen. If the probes are biased at a current of 12 μA, the probes will indicate an

electric field that points from probe A toward probe B. If the probes are biased at approximately 9 μA, the voltage difference, and hence the calculated electric field also, between the two probes is approximately half the value it is for a current bias of 12 μA. If the current bias is chosen to be approximately 6 μA, then the probes will indicate that there is very little or approximately zero electric field. In addition, if a current bias of between 0 and 5 μA is chosen, the probes will indicate an electric field that points, not from probe A toward probe B but from probe B toward probe A.

The actual electric field was negative; i.e., the plasma potential was greater when characteristic B was measured than it was when characteristic A was measured. However, if two satellite probes had characteristics similar to characteristics A and B, the magnitude and even the direction of the calculated electric field would depend on the current bias that was chosen. It is disturbing that the electric field calculated by this standard method may depend on the current bias that is chosen.

Note that it is the difference in the slopes of characteristics A and B at intermediate currents that leads to this unwanted dependence of measured electric field on bias current. Other data taken indicate that it was the difference in probe collected currents, rather than emitted currents, that was primarily responsible for this difference in slopes. Theory suggests that it is space charge that is responsible for this difference in slopes (the analysis leading to this conclusion is presented in the discussion section).

Theory

It has been known for many years [*Kingdon*, 1923] that small amounts of plasma can greatly affect the space charge near an electron emitter. Quantifying the effects that an arbitrary ambient plasma has on the space charge surrounding a particular electron emitting probe can be rather difficult, and we do not attempt to do so here. Rather, we take a more general approach to the problem. For a given probe emissivity, probe bias current, and ambient potential ϕ_A (either vacuum potential or plasma potential), i.e., for a given I_P, I_B, and ϕ_A, the voltage of a probe is minimum when the probe is in a vacuum because that is when the space charge near that probe is maximum. Likewise, for a given I_P, I_B, and ϕ_A, the voltage of a probe is maximum when the probe is in a plasma that is dense enough that the plasma ions alleviate the space charge near the probe to a level that does not impede emitted electron flow to the ambient plasma. We derive an expression for the maximum steady state space charge enhanced plasma gradient induced error in the electric field measurements taken by two identical, current biased probes by considering one of those probes to be in a near-vacuum and the other probe to be in a plasma that is dense enough that the plasma ions alleviate the space charge near the probe.

To begin our deviation of a simple expression of the maximum expected space charge enhanced PGIE, the reader is referred to Figure 5. Figure 5 shows the potential structures around two probes, the "left" probe (the probe in the near-vacuum) and the "right" probe (the probe in a plasma that is dense enough to alleviate the space charge near the probe). For simplicity the electric field in the ambient plasma has been set to zero and the potential structure of the satellite has been omitted. Also, we assume that $d_1 \sim d_2 \sim \lambda_D$, where λ_D is the Debye length of the ambient plasma.

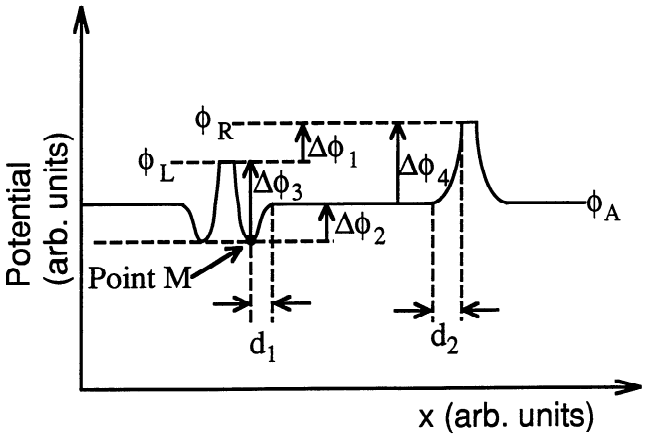

Figure 5. The qualitiative potential structure around two probes in the absence of an ambient electric field. The probe shown on the left is in a vacuum. The probe on the right is in a plasma that is dense enough to alleviate the space charge near the probe.

By inspection of Figure 5, note that $\Delta\phi_1$ is the maximum space charge enhanced PGIE. Also note from Figure 5 that if $\Delta\phi_3 = \Delta\phi_4$, then $\Delta\phi_1 = \Delta\phi_2$. In the following, we will show that $\Delta\phi_3 = \Delta\phi_4$ and give an expression for $\Delta\phi_2$ by considering the currents that flow from the probes. Note that in doing so, we will have derived an expression for the maximum space charge enhanced PGIE.

We assume steady state conditions and note that the minimum in the potential structure of the left probe (shown as point M in Figure 5) is created by space charge. If this minimum, and the potential structure of the left probe, is to stay constant with time (i.e., if $\Delta\phi_2$, $\Delta\phi_3$, and $\nabla^2\phi$ near point M are to stay constant with time), then the space charge at and near the minimum must remain constant with time. For this to happen, the current that flows from the probe to the minimum must be equal to the current that flows from the minimum to the ambient plasma (assuming, as we do, that error currents such as leakage current can be ignored). Note that the current that flows in and out of the minimum is approximately I_U (recall that this probe is in a near-vacuum for which I_C is small and will be ignored).

Now, when considering I_U to be the current associated with those electrons that are emitted from the left probe and reach to its associated potential minimum point M, I_U can be written as

$$I_U = I_P \exp(-e\Delta\phi_3/T_e) \tag{1}$$

The current I_U associated with electrons that travel from the minimum to the ambient plasma can be written (in mks units) as

$$I_U \simeq 4\varepsilon_0(e/m_e)^{1/2}\Delta\phi_2^{3/2}/\gamma \tag{2a}$$

when the probe's emission and sheath are cylindrically symmetric,

$$I_U \simeq 8\varepsilon_0(e/m_e)^{1/2}\Delta\phi_2^{3/2}/\alpha^2 \tag{2b}$$

when the probe's emission and sheath are spherically symmetric, where e and m_e are the charge and mass of an electron, γ is the ratio of the sheath radius to probe length (γ must be roughly ≤ 1 in order for probe's sheath to be

cylindrically symmetric), and α^2 is of the order of 5 and is very weakly dependent on the ratio of the probe radius to the probe's sheath thickness. Equation (2) are just the well-known Child-Langmuir law [*Langmuir and Blodgett*, 1923, 1924] rewritten in our notation for the situation depicted in Figure 5. The Child-Langmuir law describes the current flow in a vacuum from a region of zero electric field to a boundary. It is appropriate to use the Child-Langmuir law to describe the current flow from the minimum in the potential structure of the left probe to the ambient plasma because the electric field at the minimum is zero and near-vacuum conditions have been assumed at that probe. The reader may wish to note that for simplicity, we have set T_e to zero when writing the Child-Langmuir law.

PGIE, as quantitatively described by equations (5), is dependent on the current I_U. This dependence is important as it suggests that, when $I_C \ll I_U \simeq I_B$, decreasing the bias current will decrease PGIE. To those readers familiar with the Child-Langmuir law, this dependence on current rather than current density may be somewhat surprising, at least for cylindrical coordinates. Equations (5) were derived from equation (1) and the Child-Langmuir law, which in planar and cylindrical coordinates is most often written as it was originally, in terms of current density rather than current. For example, the Child-Langmuir law in cylindrical coordinates was originally written [*Langmuir and Blodgett* , 1923] as a current per unit length $i \propto V^{3/2}/r\beta^2$. Equation (2) in cylindrical coordinates was obtained by multiplying both sides of the original Child-Langmuir law by probe length L, defining γ to be r/L (where, in our case, r is the radius of the sheath of the probe), setting β^2 to 1 (β^2 ranges from 0.9990 to 1.0946 for ratios of collector (probe sheath) radius to emitter (probe) radius $\geq$11.2), and converting to mks(SI) units. As for spherical coordinates, the original Child-Langmuir law [*Langmuir and Blodgett*, 1924] was written in terms of current rather than current density and a note was made of the fact that the current was independent of the areas of both the emitter and collector.

Note that equations (2) are for cylindrically and spherically symmetric emissions. Probes in sunlight photoemit from at most half their surface area. If satellite probes were to photoemit over their entire surface areas, as is assumed when writing equations (2), then their corresponding photoemitted current would be $2I_P$ rather than I_P and (assuming a constant ratio I_U/I_P) the current associated with photoemitted electrons that reach the ambient plasma would be $2I_U$ rather than I_U. Substituting $2I_U$ for I_U in equations (2) and rearranging yields

$$I_U \simeq 2\varepsilon_0(e/m_e)^{1/2}\Delta\phi_2^{3/2}/\gamma \tag{3a}$$

when the probe's emission and sheath are cylindrically symmetric,

$$I_U \simeq 4\varepsilon_0(e/m_e)^{1/2}\Delta\phi_2^{3/2}/\alpha^2 \tag{3b}$$

when the probe's emission and sheath are spherically symmetric.

When considering I_U to be the current associated with photoemitted electrons that flow from the right probe to the plasma, I_U can be written as

$$I_U = I_P \exp(-e\Delta\phi_4/T_e) \tag{4}$$

where the I_P and T_e have been assumed to be equal to those of equation (1) because the physical characteristics of the left and right probes have been assumed to be the same. From equating equations (1) and (4) it follows that $\Delta\phi_3 = \Delta\phi_4$.

By inspection of Figure 5, the reader should see that because $\Delta\phi_3 = \Delta\phi_4$, it follows that $\Delta\phi_1 = \Delta\phi_2$. Again, by inspection of Figure 5, the reader should see that $\Delta\phi_1$ is the maximum space charge enhanced PGIE. However, $\Delta\phi_2$ is given by equations (3); and hence, because $\Delta\phi_3 = \Delta\phi_4$, the space charge enhanced PGIE can be expressed quantitatively.

Once these things are understood, it is trivial to write an expression for the maximum expected space charge enhanced PGIE from equations (3) as

$$E_M \simeq [I_U\gamma/[2\varepsilon_0(e/m_e)^{1/2}]]^{2/3}/d \tag{5a}$$

when the probe and sheath are cylindrical,

$$E_M \simeq [I_U\alpha^2/[4\varepsilon_0(e/m_e)^{1/2}]]^{2/3}/d \tag{5b}$$

when the probe and sheath are spherical, where E_M is the maximum expected error in double-probe electric field measurements due to space charge enhanced PGIE, I_U is the current associated with the photoemitted electrons that escape from and do not return to each probe of a double-probe system, γ is the ratio of the sheath radius to the probe length, and d is the distance between those two probes. Typical values of α^2 are 0.509, 1.022, 2.073, 4.002, 5.324, 6.933, and 8.523, which correspond to ratios of sheath radius to potential minimum radius of 1.8, 4.4, 14, 160, 1000, 10,000, and 100,000, respectively [*Langmuir and Blodgett*, 1924].

Equations (5) can be approximately rewritten in a more convenient form as

$$E_M(\text{mV/m}) \simeq [I_U(100\text{ nA})\gamma]^{2/3}/d(50\text{ m}) \tag{6a}$$

when the probe and sheath are cylindrical,

$$E_M(\text{mV/m}) \simeq 2[I_U(100\text{ nA})(\alpha^2/5)]^{2/3}/d(50\text{ m}) \tag{6b}$$

when the probe and sheath are spherical. The reader is reminded that $I_U = I_B - I_C$, where I_B is the bias current of a probe and I_C is the current associated with ambient particle collection by that probe. When I_C is much less than both I_U and I_B, as is often the case in tenuous plasmas, $I_U \simeq I_B$.

Figure 6 shows the theoretical characteristic assuming no space charge effects, which is labeled as 1 because it was computed using equation (1), and the theoretical characteristic assuming space charge effects, which is labeled as 3 because it was computed from equations (3) for cylindrical geometry. For computing the theoretical curves 1 and 3 shown in Figure 6, it was assumed that the ambient plasma potential ϕ_A, the emitted electron temperature T_e, the emitted current I_P, and the collected current I_C were -0.45 V, 0.28 eV, 14.8 μA, and 0.9 μA, respectively. Note that the space charge enhanced PGIE, which is proportional to the difference between these two curves, increases with increasing current.

Discussion

In Figure 7, both the experimental characteristic A of Figure 4 and the theoretical characteristics 1 and 3 of Figure 6 are shown. As can be seen by inspection of Figure 7, there

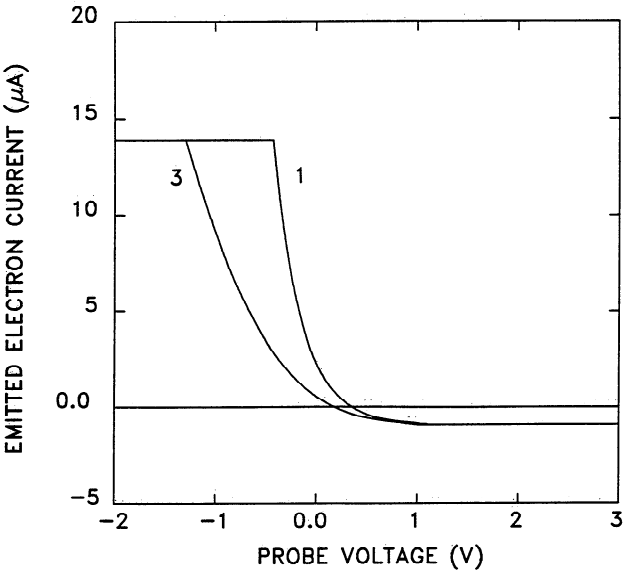

Figure 6. The theoretical characteristic assuming no space charge effects is labeled as 1 (because it was computed using equation (1)) and the theoretical characteristic assuming space charge effects is labeled as 3 (because it was computed from equation (3) for cylindrical geometry). For computing the theoretical curves 1 and 3 shown in Figure 6, it was assumed that the ambient plasma potential ϕ_A, emitted electron temperature T_e, emitted current I_P, and collected current I_C were −0.45 V, 0.28 eV, 14.8 μA, and 0.9 μA, respectively.

is quite good agreement between characteristics A and 1. This suggests that, at the time that characteristic A was measured, ϕ_A was −0.45 V and the probe's characteristic was not affected by space charge. Characteristic A was also the characteristic that was taken in the denser of the two laboratory plasmas, the plasma in which fewer space charge

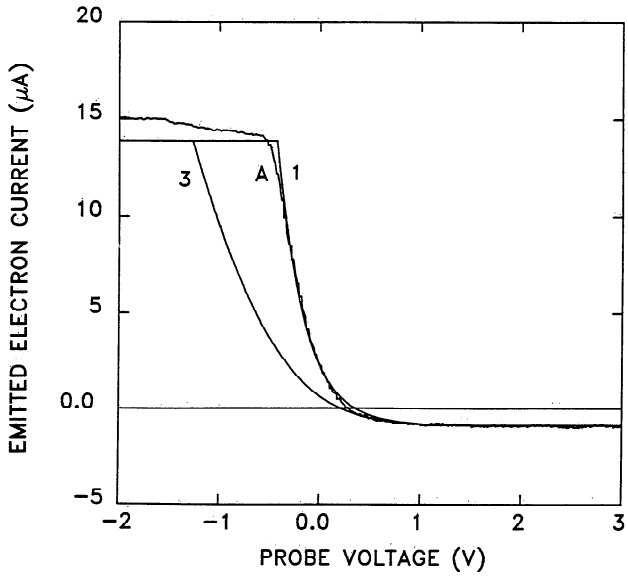

Figure 7. The experimental characteristic A of Figure 4 and the theoretical characteristics 1 and 3 of Figure 6 are shown.

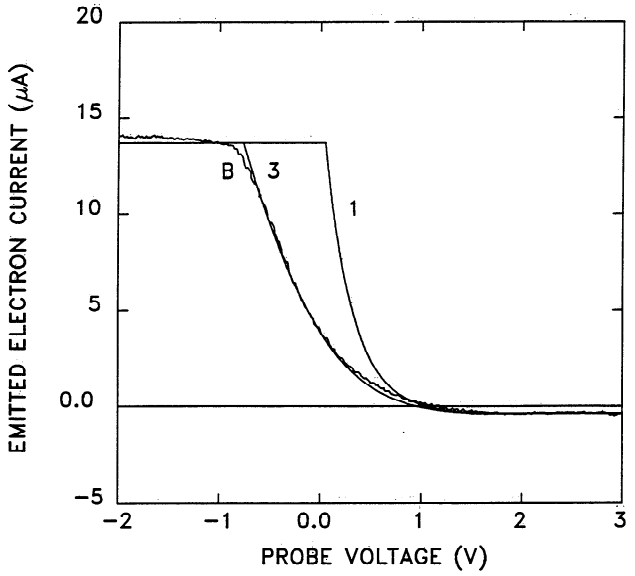

Figure 8. Both characteristic B of Figure 4 and the theoretical characteristics with ϕ_A, T_e, I_P, I_C and γ of 0.03 V, 0.28 eV, 14.1 μA, 0.4 μA, and 0.7, respectively, assumed are shown.

effects are expected because of space charge alleviation by plasma ions.

Figure 8 shows both characteristic B of Figure 4 and the theoretical characteristics with ϕ_A, T_e, I_P, I_C, and γ of 0.03 V, 0.28 eV, 14.1 μA, 0.4 μA, and 0.7, respectively, assumed. There is quite good agreement in Figure 8 between characteristics B and 3. This agreement suggests that ϕ_A was 0.03 V and space charge effects were important when characteristic B was measured. Characteristic B was taken in the more tenuous of the two laboratory plasmas, the plasma in which more space charge effects are expected because of the presence of fewer space charge alleviating plasma ions.

Together, Figures 7 and 8 suggest that the plasma potential was greater when characteristic B was measured. If characteristic 3 of Figure 6 was moved to the right by 0.48 volts, then characteristics 1 and 3 of Figure 6 would look very similar to characteristics A and B. Again, for the purposes of illustrating space charge enhanced PGIE, if characteristics A and B were those of two satellite probes of a double-probe system, the the actual electric field would point from B to A and the space charge enhanced PGIE electric field would point from probe A to B. At small bias currents (e.g., I_B = 1 to 3 μA), the space charged enhanced PGIE would be small, and the probes would measure (fairly accurately) an electric field pointing from B to A. However, at large bias currents (e.g., I_B = 11 to 13 μA), the space charged enhanced PGIE would be large, and the probes would measure (inaccurately) an electric field pointing from A to B.

Table 1 shows the error as computed from equations (5) for various satellite relevant I_U and d, with γ and α^2 set equal to 1 and 5, respectively. Table 1*a* shows the calculated errors for cylindrical probes and sheaths; Table 1*b* shows the calculated errors for spherical probes and sheaths. Note that the errors shown in Table 1*a* are less than the corresponding errors shown in Table 1*b*. By inspection of equations (5), note that for $\alpha^2/\gamma > 2$ and a given I_U and d, the maximum expected error in double probe electric field

Table 1*a*. Calculated Errors for Cylindrical Probes and Sheaths

	l_u, nA					
d, m	50	100	150	250	500	1000
20	1.77	2.81	3.68	5.18	8.22	13.0
40	0.886	1.41	1.84	2.59	4.11	6.52
60	0.590	0.937	1.23	1.73	2.74	4.35
80	0.443	0.703	0.921	1.29	2.06	3.26
100	0.354	0.562	0.737	1.04	1.64	2.61

Errors are in millivolts per meter.

measurements due to space charge enhanced PGIE is less for cylindrical probes than it is for spherical probes.

An example of satellite data that is suggestive of possible space charge enhanced PGIE is the Viking data reported by *Boström et al.* [1988] of double-probe measured electric fields that are associated with large, local depletions of the ambient plasma density. Depletions of $\Delta n/n \leq 50\%$ were observed to first pass by one probe and then the other. The electric fields associated with these density depletions were such that the voltage of the probe that was in a region of depletion at any given time was often 2 to 3 V less than the voltage of the probe that was not in the region of depletion. This is qualitatively consistent with space charge enhanced PGIE. In order to pass I_B through its sheath, the voltage of the probe in the region of the density depletion would have to be less than that of the other probe if the density depletion caused the space charge near it to be greater than the space charge near the other probe.

Although Viking data reported by *Boström et al.* [1988] is in qualitative agreement with space charge enhanced PGIE, it is not in quantitative agreement. The distance between the spherical probes of Viking is approximately 80 m. But when Viking probes are operated for electric field measurements rather than density measurements, they are typically current biased to only approximately 150 nA [*Boström*, 1991]. As can be seen from Table 1, for these parameters, the theory predicts a maximum space charge enhanced PGIE that is more than an order of magnitude less than the observed electric field of approximately 2.5 V/80 m or 30 mV/m. Hence it seems fairly certain that the Viking results referred to are not dominated by space charge enhanced PGIE.

Last, the reader should beware that although we derive an expression for maximum space charge enhanced PGIE, we do not take into account many things which might change that maximum error. Among the effects that we do not take into account are: most particularly, transient effects, i.e., gradients which pass by the probes quickly enough that their effects are capacitively coupled to the probes; energetic particles [*Temerin et al.*, 1982]; charge exchange effects [*Intrator et al.*, 1988]; the nonzero temperatures of emitted electrons; distance of the potential minima from the probes; magnetic fields; probe nonuniformity; and leakage currents. Nonzero emitted electron temperature and position of the potential minima will tend to reduce the maximum space charge enhanced error. Our laboratory probe thermionically emitted electrons, and hence the error shown by our probe will tend to be greater than the corresponding error of satellite probes because of the relatively low temperature (approximately 0.3 eV) of thermionically emitted electrons as compared to photoemitted electrons (approximately a few electron volts). For cylindrical geometry there's an approximately 25% and 40% reduction in the error for $T_e = 1$ and 4 eV, respectively [*Langmuir and Blodgett*, 1923]. Magnetic fields, probe nonuniformity, and leakage currents will tend to increase the maximum error; but as noted in the Introduction, techniques are generally employed to reduce these latter two phenomena. Magnetic fields are probably not a concern unless they are strong enough that $2r_{g,e} \simeq \lambda_D$, where $r_{g,e}$ is the emitted electron gyroradius.

Table 1*b*. Calculated Errors for Spherical Probes and Sheaths

	l_u, nA					
d, m	50	100	150	250	500	1000
20	3.26	5.18	6.79	9.54	15.1	24.0
40	1.63	2.59	3.39	4.77	7.57	12.0
60	1.09	1.73	2.26	3.18	5.05	8.01
80	0.816	1.29	1.70	2.38	3.79	6.01
100	0.652	1.04	1.36	1.91	3.03	4.81

Errors are in millivolts per meter.

Appendix A

The measuring of probe current versus voltage characteristics was complicated by the finite impedance between the primary and secondary of the heating voltage transformer. Figure A1 is a schematic of the electrical components that

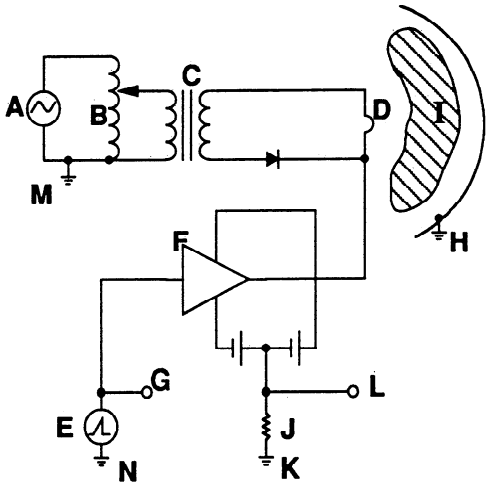

Figure A1. An electrical schematic of the probe heating circuit, the probe, the plasma, the plasma boundary, the probe bias circuit, and the probe current diagnostic. Component *A* represents the line voltage (120 V, 60 Hz), component *B* is a variac or variable voltage transformer, *C* is an isolation transformer, *D* is the probe, *E* is a voltage ramp, *F* is the voltage follower through which the voltage ramp is applied to the probe, *G* is the point at which the bias voltage of the probe is measured, *H* is the vacuum vessel wall and its ground, *I* is the vacuum or plasma between the probe and vacuum vessel wall, *J* is a resistor, and *L* is the point at which a voltage equal to the current flowing through the probe multiplied by the resistance of *J* is measured.

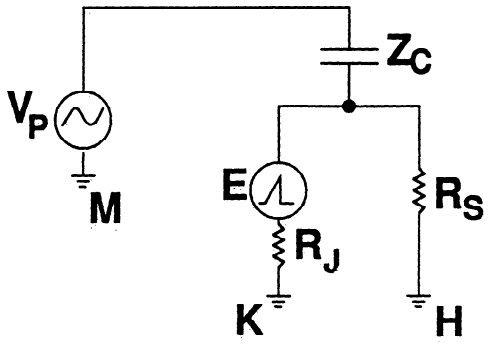

Figure A2. A simplified approximation of Figure A1 that depicts the circuit elements that lead to an unwanted current across the isolation transformer. Specifically, Z_C is the impedance, which is due to the finite capacitance across the transformer, R_J is the resistance of resistor J, R_S is the "sheath" or approximate resistance between the probe D and ground H, and V_P is the voltage across the primary winding of the isolation transformer C.

are pertinent to this discussion. Components A through C provide the voltage that heats the probe D into thermionic emission. Component A represents the line voltage (120 V, 60 Hz), B is a variac or variable voltage transformer, and C is an isolation transformer. Component E is a voltage ramp (that is, a voltage with respect to ground that increases linearly with time) which is applied to the probe through the voltage follower F. G is the point at which the "probe voltage" or "bias voltage of the probe" is measured. Component H represents the vacuum vessel wall and its ground. I depicts the vacuum or plasma that lies between the probe and vacuum vessel wall.

Note that there are four grounds, M, H, K, and N. The current that we are interested in, the current which is supposed to correspond to the current in a probe's current versus voltage characteristic, is the current that flows between the probe D and the ground H. The impedance between the probe D and the ground N should be quite large; it should be of the order of the input resistance of the voltage follower F, which is a CA3140 op amp and has a nominal input resistance of $10^{12}\Omega$. Ideally, the impedance between the probe D and ground M is also quite large because of the large impedance between the primary and secondary of the isolation transformer C. In this case, the current that flows from ground H to probe D completes its circuit by flowing from probe D through the voltage follower F and the resistor J to ground K. The current through the probe is then calculated by dividing the voltage measured at point L by the resistance of J.

Unfortunately, the impedance between the primary and secondary of our isolation transformer C is small enough to allow significant current to flow between ground M and grounds H and K. In fact, during most times in the heating cycle, the current flowing to our ground K is dominated by current flowing from M through C, F, and J to K and not by the current that we wish to measure which is the current that flows from H through I, D, F, and J to K.

There are two types of impedance across C that are of concern, capacitance and resistance. There is finite capacitance between the primary and secondary windings of C because of their proximity to one another. Figure A2 is a simplified approximation of Figure A1 and depicts the circuit elements essential in understanding how we avoid the problem caused by the capacitance across the isolation transformer. V_P in Figure A2 corresponds to the voltage across the primary of the isolation transformer, and Z_C is the value of the impedance due to the finite capacitance across the transformer. E is a voltage sweep of the same value as the voltage sweep depicted in Figure A1 and represents the output of the voltage follower F, R_J is the resistance of the resistor J, and R_S is the "sheath" resistance or the approximate resistance between the probe D and the ground H.

It is common practice to make R_J much less than R_S, and Z_C is usually much greater than either R_J or R_S. In other words,

$$Z_C \gg R_S \gg R_J \tag{A1}$$

Hence most of the current that flows from ground M flows to ground K and not to ground H. Also, the phase of this cyclical current proceeds V_P by $\pi/4$; the current passes through zero when V_P passes through its maximum and minimum. We can essentially eliminate the effect of this unwanted current on our measurements of probe current versus voltage characteristics by monitoring V_P and triggering a temporally short voltage pulse at the minimum of each cycle of V_P. This voltage pulse is in turn used to trigger a linear gate, which samples the voltage at point L in Figure A1 during (and only during) the voltage pulse. In this way, data are sampled periodically at a time in the cycle of the unwanted current when the amplitude of the current is near zero.

There is also a finite resistive impedance across the isolation transformer C. The resistance across our particular transformer only becomes troublesome when the heating voltage is applied to the probe for over 20 s. It is our conjecture that with time the transformer becomes warm, the resistance across C decreases, and as a result the current across the resistance increases and starts to be noticeable on the measured current versus voltage characteristic.

Our solution to this problem is to simply measure the characteristics quickly, before there is a noticeable resistive current. There are of course limits as to how quickly the characteristics can be measured. We have noticed that the emitted current continues to increase for the first few seconds after the heating voltage is applied before leveling off to a constant value. Presumably, the probe is warming up during these first few seconds. Note that the warming takes place immediately after the heating voltage is applied to the probe while the resistance does not become too small for making measurements until some time after. Further, these two currents are of opposite sign, that is, warming increases the emitted current while the finite resistance decreases the measured emitted current (because some of the emitted current flows through ground M rather than ground K). Hence we have a check on these two effects. We measure each characteristic twice, with enough time between the measurements to allow the transformer to cool down. The first characteristic is measured by sweeping the probe from low to high voltage; the second characteristic is measured by sweeping from high to low. The measurement is good when there is good agreement between the two characteristics. When the warming of the probe and/or the warming of the transformer is a problem, the two characteristics do not

agree at either low and/or high voltages, that is, at either early and/or late times in the sweeps.

If our conjecture is correct that the resistance across the transformer decreases with time as the transformer heats up, an increase in the size the transformer might help by increasing the time it takes the transformer to warm up. However, increasing the size would probably also increase the capacitance between the primary and the secondary. An increase in this capacitance would make the problem of finite capacitive impedance more acute.

As noted in the text, plasma cannot be produced in the 10^{-4} torr range until it is first produced in the 10^{-3} torr range. However, once plasma is produced in the 10^{-3} torr range, the heating voltage to the filament is turned off for a minute or so. This is to allow the transformer to cool down and to allow time for the pressure to be lowered into the 10^{-4} torr range. It is fortunate, although not well understood by us, that plasma can still be produced in the 10^{-4} torr range once it has been produced in the 10^{-3} torr range even when some time has passed without production. If approximately five or more minutes are allowed to pass, then plasma must once again be produced in the 10^{-3} torr range before it can be produced in the 10^{-4} torr range.

Acknowlegments. We thank T. Aggson, N. Maynard, and R. Pfaff for their encouragement, support, and many useful conversations. We also thank R. Boström and F. Mozer for useful discussions and J. Meyer for his assistance in preparing the figures. This work was supported by NASA Goddard NAG 5-1135 and NSF grant ATM-901751.

The Editor thanks two referees for their assistance in evaluating this paper.

References

Aggson, T. L., and J. P. Heppner, A proposal for electric field measurements on ATS-1, Goddard Space Flight Cent., Greenbelt, Md., July 1964.

Aggson, T. L., B. G. Ledley, A. Egeland, and I. Katz, Probe measurements of DC electric fields, in Proceedings of the 17th ESLAB Symposium, *Eur. Space Agency, Spec. Publ., ESA SP-198*, 13, 1983.

Borovsky, J. E., The theory of Langmuir probes in strong electrostatic potential structures, *Phys. Fluids*, *29*, 718, 1986.

Boström, R., G. Gustafsson, B. Holback, G. Holmgren, H. Koskinen, and P. Kintner, Characteristics of solitary waves and weak double layers in the magnetospheric plasma, *Phys. Rev. Lett.*, *61*, 82, 1988.

Boyd, R. L. F., Measurement of electric fields in the ionosphere and magnetosphere, *Space Sci. Rev.*, *7*, 230, 1967.

Fahlesson, U., Theory of electric field measurements conducted in the magnetosphere with electric probes, *Space Sci. Rev.*, *7*, 238, 1967.

Fehringer, M., Double-spin probe potential modulations in the electric field experiment, internal report of the Space Sci. Dept., Eur. Space Res. and Technol. Cent. (ESTEC), Noordwilk, Netherlands, April 1989.

Guernsey, R. L., and J. H. M. Fu, Potential distribution surrounding a photo-emitting plate in a dilute plasma, *J. Geophys. Res.*, *75*, 3193, 1970.

Gurnett, D. A., Plasma wave electric field measurements, *Eos Trans. AGU*, *72*(44), Fall Meeting Suppl., 409, 1991.

Intrator, T., M. H. Cho, E. Y. Wang, N. Hershkowitz, D. Diebold, and J. DeKock, The virtual cathode as a transient double sheath, *J. Appl. Phys.*, *64*, 2927, 1988.

Kingdon, K. H., A method for the neutralization of electron space charge by positive ionization at very low gas pressures, *Phys. Rev., Ser. II*, *21*, 408, 1923.

Langmuir, I., and K. Blodgett, Currents limited by space charge between coaxial cylinders, *Phys. Rev., Ser. II*, *22*, 347, 1923.

Langmuir, I., and K. Blodgett, Currents limited by space charge between concentric spheres, *Phys. Rev., Ser. II*, *24*, 49, 1924.

Mozer, F. S., R. B. Torbert, U. V. Fahleson, C. G. Falthammar, A. Gonfalone, and A. Pedersen, Measurements of quasi-static and low-frequency electric fields with spherical double probes on the ISEE-1 spacecraft, *IEEE Trans. Geosci. Electron.*, *GE-16*, 258, 1978.

Pedersen, A., R. Grard, K. Knott, D. Jones, A. Gonfalone, and U. Fahleson, Measurements of quasi-static electric fields between 3 and 7 radii on GEOS-1, *Space Sci. Rev.*, *22*, 333, 1978.

Pedersen, A., C. A. Cattell, C. G. Falthammar, V. Formisano, P. A. Lindqvist, F. Mozer, and R. Torbert, Quasistatic electric field measurements with spherical double probes on the GEOS and ISEE satellites, *Space Sci. Rev.*, *37*, 269, 1984.

Temerin, M., K. Cerney, W. Lotko, and F. S. Mozer, Observations of double layers and solitary waves in the auroral plasma, *Phys. Rev. Lett.*, *48*, 1175, 1982.

J. R. DeKock, D. A. Diebold, N. Hershkowitz, T. P. Intrator, and S-G. Lee, Department of Nuclear Engineering and Engineering Physics, University of Wisconsin, Madison, WI 53706.

M-K. Hsieh, Department of Electrical and Computer Engineering, University of Wisconsin, Madison, WI 53706.

(Received February 24, 1992; revised February 8, 1993; accepted February 10, 1993.)